# Supplementary Information

**Direct Carbonization of Black Liquor Powders into 3D Honeycomb-Like Porous Carbons with Tunable Disordered Degree for Sodium-Ion Battery**

Jianyu Huang,[1, 2] Weicai Zhang,[1, 2] Peifeng Yu,[1, 2] Hanwu Dong,[1, 2] Mingtao Zheng,[1, 2] Yong Xiao,[1, 2] Hang Hu,[1, 2] Yingliang Liu,[*1, 2] Yeru Liang[*1, 2]

*1. Key Laboratory for Biobased Materials and Energy of Ministry of Education/Guangdong Provincial Engineering Technology Research Center for Optical Agriculture, College of Materials and Energy, South China Agricultural University, Guangzhou, 510642, China.*

*2. Guangdong Laboratory of Lingnan Modern Agriculture, Guangzhou, 510642, China.*

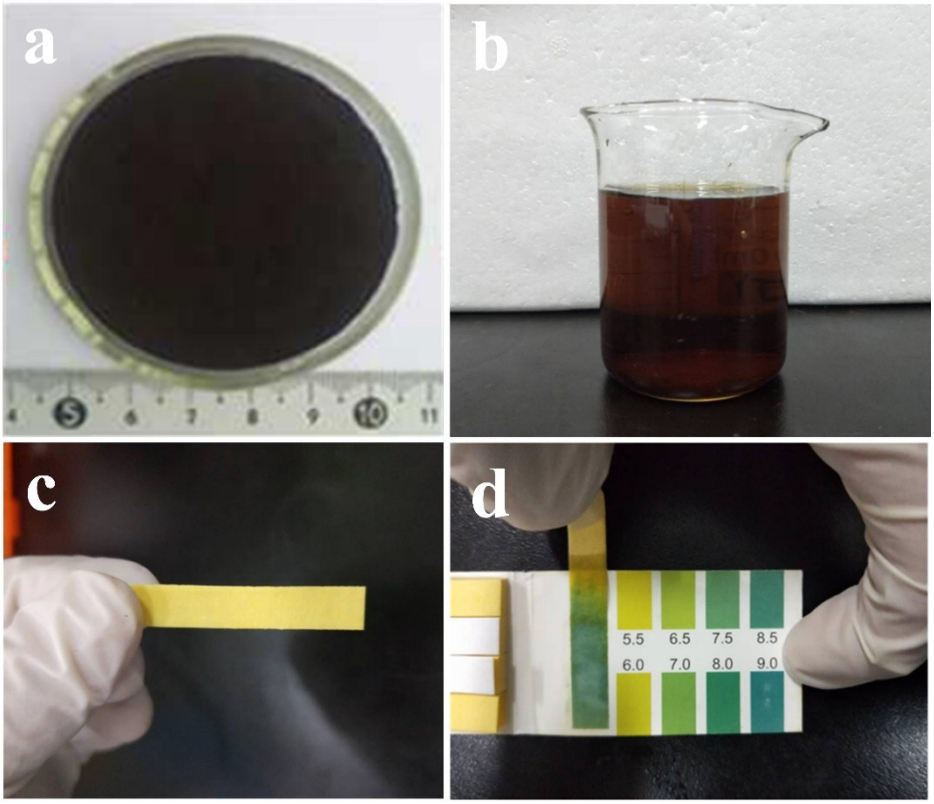


**Fig. S1** Photographs of (a) the black liquid powder, (b) the black liquid aqueous solution, pH test paper without (c) and with (d) the addition of black liquid.

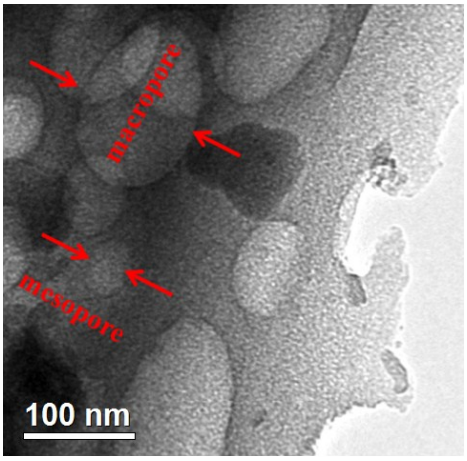


**Fig. S2** TEM image of the BL-PC-1.

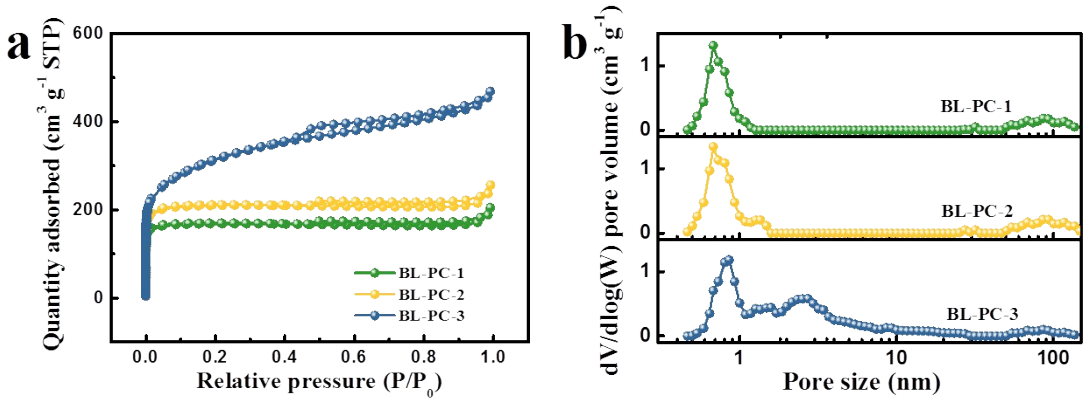


**Fig. S3** (a) $N_2$ adsorption–desorption isotherms and (b) DFT pore size distribution curves of the typical samples.

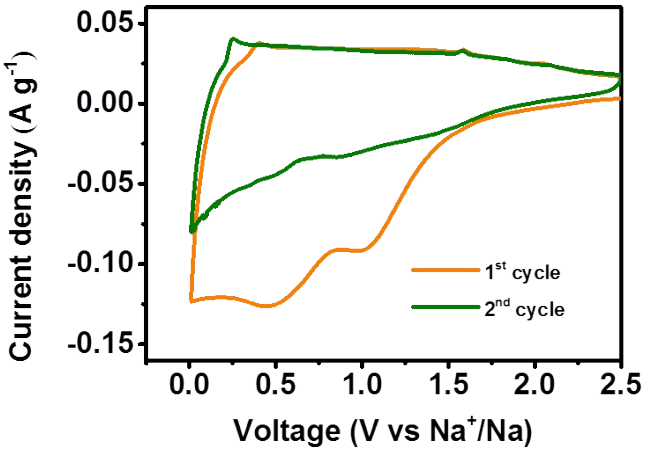


**Fig. S4** CV curves of BL-PC-1 for the first two cycles for at a scan rate of 0.1mV $s^{-1}$.

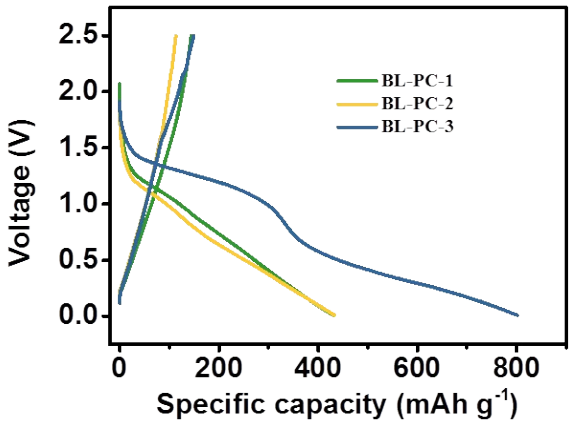


**Fig. S5** Galvanostatic charge–discharge curves for the first discharge/charge profile of BL-PC-1, BL-PC-2 and BL-PC-3 at a current density of 100 mA $g^{-1}$.

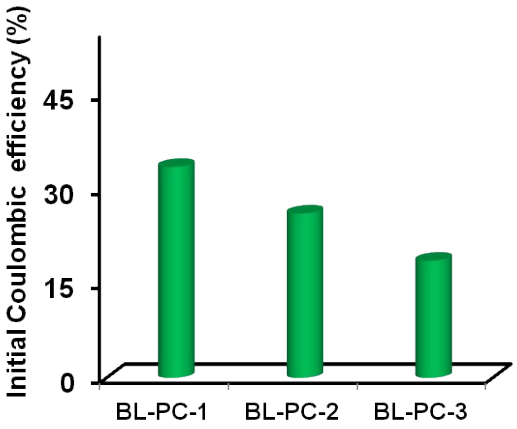


**Fig. S6** The initial Coulombic efficiency for the BL-PCs.

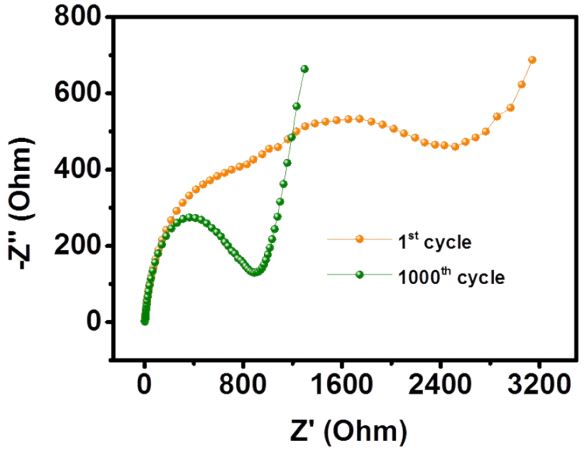


**Fig. S7** Electrochemical impedance spectra of the BL-PC-1.

**Table S1** Summary of BET specific surface area and total pore volume of the samples.

| Samples | $S_{BET}$ ($m^2$ $g^{-1}$) | $V_t$ ($cm^3$ $g^{-1}$) |
|---|---|---|
| BL-PC-1 | 683 | 0.27 |
| BL-PC-2 | 829 | 0.33 |
| BL-PC-3 | 1146 | 0.72 |

**Table S2** Electrochemical performance comparison of various anodes materials for sodium-ion batteries

| Samples | Capacity (mAh $g^{-1}$) at high current density | Range of current density (mA $g^{-1}$) | Capacity retention (%) | Refer. number |
|---|---|---|---|---|
| **BL-PC-1** | **83 (1000 mA $g^{-1}$)** | **100-1000** | **60** | **This work** |
| Hard carbon | 50 (1000 mA $g^{-1}$) | 50-1000 | 22 | [1] |
| Porous hard carbons | 75 (500 mA $g^{-1}$) | 40-500 | 28 | [2] |
| Sugar-derived carbons | 62 (1000 mA $g^{-1}$) | 100-1000 | 28 | [3] |
| Reed straw derived hard carbon | 46 (1000 mA $g^{-1}$) | 100-1000 | 22 | [4] |
| Water caltrop shell-derived hard carbons | 51 (1000 mA $g^{-1}$) | 100-1000 | 18 | [5] |
| Hierarchically porous carbon monoliths | 63 (1000 mA $g^{-1}$) | 100-1000 | 58 | [6] |
| Mesocarbon microbeads | 30 (800 mA $g^{-1}$) | 100-800 | 13 | [7] |
| Hierarchical porous carbons | 105 (1000 mA $g^{-1}$) | 100-1000 | 60 | [8] |
| Reduced graphene oxide | 96 (1000 mA $g^{-1}$) | 80-1000 | 54 | [9] |
| Hollow carbon sphere | 120 (1000 mA $g^{-1}$) | 200-1000 | 54 | [10] |
| Hollow carbon nanowires | 149 (500 mA $g^{-1}$) | 50-500 | 59 | [11] |
| Carbon nanoparticle | 78 (1000 mA $g^{-1}$) | 100-1000 | 28 | [12] |
| Surface-carboxylated carbon nanoparticles | 82 (1000 mA $g^{-1}$) | 100-1000 | 30 | [12] |
| Carbon nanotubes | 36 (1000 mA $g^{-1}$) | 100-1000 | 52 | [13] |
| Carbon nanosheets | 80 (1000 mA $g^{-1}$) | 100-1000 | 23 | [14] |
| Microporous spherical carbon | 67 (1000 mA $g^{-1}$) | 100-1000 | 51 | [15] |
| Carbon nanofibers | 75 (1000 mA $g^{-1}$) | 100-1000 | 34 | [16] |
| Crumpled graphene paper | 100 (1000 mA $g^{-1}$) | 100-1000 | 59 | [17] |
| Hard carbon nanoparticles | 72 (1250 mA $g^{-1}$) | 125-1250 | 31 | [18] |

| | | | | |
|---|---|---|---|---|
| Lignin-derived carbon | 75 (1000 mA $g^{-1}$) | 100-1000 | 50 | [3] |
| Oak sawdust-derived | 3.5 (1000 mA $g^{-1}$) | 100-1000 | 1.9 | [3] |
| Densified graphene | 91 (1000 mA $g^{-1}$) | 100-1000 | 72 | [19] |
| Hard carbon derived from cucumber stem | 73 (1000 mA $g^{-1}$) | 100-1000 | 31 | [20] |
| Hard carbon | 52 (1000 mA $g^{-1}$) | 100-1000 | 32 | [21] |
| Kraft lignin/ cellulose acetate derived carbon powder | 50 (500 mA $g^{-1}$) | 50-500 | 29 | [22] |
| Kraft lignin derived carbon powder | 42 (500 mA $g^{-1}$) | 50-500 | 23 | [22] |
| Cellulose acetate nanofibers | 19 (500 mA $g^{-1}$) | 50-500 | 32 | [22] |
| Hard carbon microspherules | 78 (600 mA $g^{-1}$) | 60-600 | 30 | [23] |
| Metal organic framework-derived carbons | 85 (200 mA $g^{-1}$) | 50-200 | 53 | [24] |
| Mesoporous disordered carbon | 115 (1000 mA $g^{-1}$) | 100-1000 | 40 | [25] |
| Mesoporous soft carbon | 105 (1000 mA $g^{-1}$) | 100-1000 | 47 | [26] |
| Porous Carbon/Sn composite | 80 (1000 mA $g^{-1}$) | 100-1000 | 32 | [27] |
| Sn/micron-sized disordered carbon | 90 (610 mA $g^{-1}$) | 12-610 | 50 | [28] |
| Sn thin film on conductive wood fiber | 50 (170 mA $g^{-1}$) | 84-170 | 38 | [29] |
| Trisodium 1,2,4-benzenetricarboxylate | 53 (400 mA $g^{-1}$) | 50-400 | 28 | [30] |
| paracyclophane-1,9,17,25-tetraene | 70 (1000 mA $g^{-1}$) | 100-1000 | 47 | [31] |
| Sodium Naphthalene Dicarboxylate | 85 (500 mA $g^{-1}$) | 31-500 | 40 | [32] |

# References:


[1]. Xiao, B., et al., Lithium-Pretreated Hard Carbon as High-Performance Sodium-Ion Battery Anodes. Advanced Energy Materials, 2018. 8(24): p. 1801441.

[2]. Zhang, N., et al., High capacity hard carbon derived from lotus stem as anode for sodium ion batteries. Journal of Power Sources, 2018. 378: p. 331-337.

[3]. Yoon, D., et al., Carbon with Expanded and Well-Developed Graphene Planes Derived Directly from Condensed Lignin as a High-Performance Anode for Sodium-Ion Batteries. ACS Applied Materials & Interfaces, 2017. 10(1): p. 569-581.

[4]. Wang, J., et al., Facile hydrothermal treatment route of reed straw-derived hard carbon for high performance sodium ion battery. Electrochimica Acta, 2018. 291: p. 188-196.

[5]. Wang, P., et al., Low-cost water caltrop shell-derived hard carbons with high initial coulombic efficiency for sodium-ion battery anodes. Journal of Alloys and Compounds, 2019. 775: p. 1028-1035.

[6]. Gong, J., et al., A Novel Method of Fabricating Free-Standing and Nitrogen-Doped 3D Hierarchically Porous Carbon Monoliths as Anodes for High-Performance Sodium-Ion Batteries by Supercritical CO2 Foaming. ACS Applied Materials & Interfaces, 2019.

[7]. Song, L., et al., Anode performance of mesocarbon microbeads for sodium-ion batteries. Carbon, 2015. 95: p. 972-977.

[8]. Wang, H., et al., Biomass derived hierarchical porous carbons as high-performance anodes for sodium-ion batteries. Electrochimica Acta, 2016. 188: p. 103-110.

[9]. Wang, Y., et al., Reduced graphene oxide with superior cycling stability and rate capability for sodium storage. Carbon, 2013. 57: p. 202-208.

[10]. Tang, K., et al., Hollow Carbon Nanospheres with Superior Rate Capability for Sodium-Based Batteries. Advanced Energy Materials, 2012. 2(7): p. 873-877.

[11]. Cao, Y., et al., Sodium Ion Insertion in Hollow Carbon Nanowires for Battery Applications. Nano Letters, 2012. 12(7): p. 3783-3787.

[12]. Gaddam, R.R., et al., Biomass derived carbon nanoparticle as anodes for high performance sodium and lithium ion batteries. Nano Energy, 2016. 26: p. 346-352.

[13]. Luo, X., et al., Graphene nanosheets, carbon nanotubes, graphite, and activated carbon as anode materials for sodium-ion batteries. Journal of Materials Chemistry A, 2015. 3(19): p. 10320-10326.

[14]. Wang, H., et al., Nitrogen-Doped Porous Carbon Nanosheets as Low-Cost, High-Performance Anode Material for Sodium-Ion Batteries. ChemSusChem, 2013. 6(1): p. 56-60.

[15]. Zhou, D., et al., Long cycle life microporous spherical carbon anodes for sodium-ion batteries derived from furfuryl alcohol. JOURNAL OF MATERIALS CHEMISTRY A, 2016. 4(17): p. 6271-6275.

[16]. Zhao, P., et al., Electrochemical performance of fulvic acid-based electrospun hard carbon nanofibers as promising anodes for sodium-ion batteries. Journal of Power Sources, 2016. 334: p. 170-178.

[17]. Yun, Y.S., et al., Crumpled graphene paper for high power sodium battery anode. Carbon, 2016. 99: p. 658-664.

[18]. Xiao, L., et al., Hard carbon nanoparticles as high-capacity, high-stability anodic materials for Na-ion batteries. Nano Energy, 2016. 19: p. 279-288.

[19]. Zhang, J., et al., The Interplay of Oxygen Functional Groups and Folded Texture in Densified Graphene Electrodes for Compact Sodium-Ion Capacitors. Advanced Energy Materials, 2018. 8(11): p. 1702395.

[20]. Li, C., et al., Heteroatom-doped hierarchically porous carbons derived from cucumber stem as high-performance anodes for sodium-ion batteries. Journal of Materials Science, 2019. 54(7): p. 5641-5657.

[21]. Liu, X., et al., High Capacity and Cycle-Stable Hard Carbon Anode for Nonflammable Sodium-Ion Batteries. ACS Applied Materials & Interfaces, 2018. 10(44): p. 38141-38150.

[22]. Jia, H., et al., Electrospun Kraft Lignin/Cellulose Acetate-Derived Nanocarbon Network as an Anode for High-Performance Sodium-Ion Batteries. ACS Applied Materials & Interfaces, 2018. 10(51): p. 44368-44375.

[23]. Li, Y., et al., Amorphous monodispersed hard carbon micro-spherules derived from biomass as a high performance negative electrode material for sodium-ion batteries. Journal of Materials Chemistry A, 2015. 3(1): p. 71-77.

[24]. Ingersoll, N., et al., Metal organic framework-derived carbon structures for sodium-ion battery anodes. Electrochimica Acta, 2019. 297: p. 129-136.

[25]. Raj K, A., et al., Bio-derived mesoporous disordered carbon: An excellent anode in sodium-ion

battery and full-cell lab prototype. Carbon, 2019. 143: p. 402-412.
[26]. Cao, B., et al., Mesoporous soft carbon as an anode material for sodium ion batteries with superior rate and cycling performance. Journal of Materials Chemistry A, 2016. 4(17): p. 6472-6478.
[27]. Xu Y., et al., Electrochemical Performance of Porous Carbon/Tin Composite Anodes for Sodium-Ion and Lithium-Ion Batteries. Adv Energy Mater, 2013: p. 128-133.
[28]. Bresser D., et al., Embedding tin nanoparticles in micron-sized disordered carbon for lithium- and sodium-ion anodes. Electrochim Acta, 2014. 128: p. 163-71.
[29]. Zhu H., et al., Tin Anode for Sodium-Ion Batteries Using Natural Wood Fiber as a Mechanical Buffer and Electrolyte Reservoir. Nano Lett 2013, 13: p. 3093-3100.
[30]. Luo C, Shea JJ, Huang J. A carboxylate group-based organic anode for sustainable and stable sodium ion batteries. J Power Sources 2020, 453: p. 227904.
[31]. Eder S., et al. Switching between local and global aromaticity in a conjugated macrocycle enables high‐performance organic sodium‐ion battery anodes. Angewandte Chemie International Edition, 2020. Doi.org/10.1002/anie.202003386.
[32]. Medabalmi V., et al., Sodium Naphthalene Dicarboxylate Anode Material for Inorganic-Organic Hybrid Rechargeable Sodium-Ion Batteries. J Electrochem Soc, 2018, 165: p. A175-A180.